British Journal of Pharmacology (2006) 148, 814–824
www.nature.com/bjp

Citrobacter rodentium-induced NF-κB activation in hyperproliferating colonic epithelia: role of p65 (Ser^{536}) phosphorylation

[1]Yu Wang, [1]Guang-Sheng Xiang, [1]Famourou Kourouma & *,[1]Shahid Umar

[1]Division of Gastroenterology and Hepatology, Department of Internal Medicine, University of Texas Medical Branch, 301 University Blvd, 1108 Strand, Galveston TX 77555-0632, U.S.A.

1 The transcription factors of the NF-κB/Rel family form dimeric complexes that control expression of various genes involved in inflammation and proliferation.

2 During transmissible murine colonic hyperplasia (TMCH) induced by *Citrobacter rodentium*, nuclear translocation of NF-κB in isolated colonic crypts increased 3 day's post-infection and continued over 12 days paralleling peak hyperplasia. Antibody supershifts for both p65/p50 hetero- and p50/p50 homodimers occurred. Expression levels of both p50 and p65 subunits increased in cytosolic/nuclear extracts and correlated with NF-κB activation kinetics. IκBα levels decreased during this time.

3 Phosphorylation of IKKα (at Ser$^{176/180}$) and -β (at Ser$^{177/181}$) increased significantly during TMCH suggesting activation *in vivo*.

4 p65-Ser^{536} (p65^{536}) exhibited increased phosphorylation on immunoblotting and immunohistochemistry (IHC) both at day 6 and 12 TMCH. p65^{536} translocated to nucleus and interacted with transcriptional coactivator CREB binding protein (CBP).

5 Proteasomal inhibitor bortezomib (Velcade®) caused accumulation of Ser$^{32/36}$-phosphorylated IκBα and significant inhibition of NF-κB activity *in vivo*. Velcade® also blocked nuclear translocation of activated p65: both immunoblotting and IHC failed to detect p65^{536} nuclear immunoreactivity. Velcade®, however, did not abrogate TMCH.

6 p65 interacted strongly with ribosomal S6 kinase 1 (RSK-1) during coimmunoprecipitation but not with IKKα or -β.

7 Thus, NF-κB activation during TMCH involves both IκBα degradation and p65-Ser^{536} phosphorylation. p65/RSK-1 interaction and concomitant increase in p65^{536} complexed with CBP may be important in modulating NF-κB activity *in vivo*. Activated NF-κB, besides modulating proliferation, may aid in providing protective immunity against *C. rodentium* infection *in vivo*.
British Journal of Pharmacology (2006) **148,** 814–824. doi:10.1038/sj.bjp.0706784;
published online 5 June 2006

Keywords: *in vivo*; *C. rodentium*; colon; hyperproliferation; hyperplasia; NF-κB

Abbreviations: DAB, diaminobenzidine; IKK, IκB kinase; MEK, mitogen-activated protein kinase kinase; NF-κB, nuclear factor-kappa B; SCID, severe combined immune deficiency; TMCH, transmissible murine colonic hyperplasia

Introduction

Transmissible murine colonic hyperplasia (TMCH) is a disease of mice characterized by significant epithelial cell proliferation and variable degrees of inflammation and necrosis, depending upon the genetic background (Barthold *et al*., 1976; Barthold *et al*., 1978; Brenner *et al*., 1993; Schauer *et al*., 1995). The causative agent *Citrobacter rodentium* (*C. rodentium*), is a natural non-invasive bacterial pathogen which infects the distal colon of mice. It uses the same molecular mechanisms of type III secretion as human enteropathogenic (EPEC) and enterohemorrhagic *Escherichia coli* (EHEC) to colonize the epithelial cells of the gut (Kenny *et al*., 1996; Goosney *et al*., 2000; Donnenberg & Whittam, 2001). In Swiss outbred adult mice, the response is almost purely proliferative with minimal inflammation suggesting that such an axis if present resolves quickly (Barthold *et al*., 1976; Barthold *et al*., 1978; Brenner *et al*., 1993; Schauer *et al*., 1995). *C. rodentium* infection in young mice produces pathology and elicits a mucosal T_h-1 immune response very similar to mouse models of inflammatory bowel diseases (Higgins *et al*., 1999). These proinflammatory responses are regulated by activation of a key inflammatory marker, NF-κB. However, unlike studies where EPEC and EHEC infections trigger activation of NF-κB and subsequent modulation of the proinflammatory gene expression, it is not known whether *C. rodentium* infection induces NF-κB activation *in vivo*.

Many of the chemokines, cytokines and innate defense molecules produced by intestinal epithelial cells in response to bacterial infection are target genes of NF-κB (Hobbie *et al*., 1997; Savkovic *et al*., 1997; Elewaut *et al*., 1999; O'neil *et al*.,

*Author for correspondence; E-mail: shumar@utmb.edu

1999; Philpott *et al*., 2000). NF-κB appears to be a central regulator of the epithelial cell innate immune response to infection by a spectrum of bacteria that use different strategies to adhere to and invade intestinal epithelial cells (Elewaut *et al*., 1999). NF-κB is a dimeric transcription factor composed of homodimers and heterodimers of Rel proteins, of which there are five family members in mammalian cells (i.e., RelA (p65), c-Rel, RelB, NF-κB1 (p50), and NF-κB2 (p52)) (Baeuerle, 1991; Baeuerle & Henkel, 1994). NF-κB dimers are held in the cytoplasm in an inactive state by inhibitory proteins, the IκBs. IκB proteins include IκBα, IκBβ, IκBε, p105 and p100. NF-κB activation entails the signal-induced phosphorylation and degradation of IκB molecules, which in turn releases NF-κB to translocate into the nucleus and bind to response elements of target promoters (Beg *et al*., 1993; Henkel *et al*., 1993; Scherer *et al*., 1995; DiDonato *et al*., 1997; Lee *et al*., 1997; Mercurio *et al*., 1997; Zandi *et al*., 1997). The various NF-κB subunits and IκBs enable the cell to modulate NF-κB responses in a highly controlled manner.

NF-κB can be activated *via* distinct pathways. The commonest, called the classical pathway, triggered in response to microbial or proinflammatory cytokine insult, leads to recruitment and activation of the IκB-kinase (IKK) complex which includes the scaffold protein NF-κB essential modulator (NEMO; also named IKKγ), IKKα and IKKβ kinases (Zandi *et al*., 1997). Once activated, IKK complex phosphorylates NF-κB-bound IκBs and targets them for ubiquitination-dependent degradation. IκB phosphorylation depends mainly on the IKKβ catalytic subunit of the IKK complex (Li *et al*., 1999a, b).

IκBα degradation is incomplete and delayed in intestinal epithelial cells, resulting in buffered responses to luminal stimuli. The stimulatory environment partially determines whether the effect of NF-κB is protective or deleterious for the host. κB-dependent proinflammatory gene expression, particularly chemokines, major histocompatibility complex class II antigens and adhesion molecules may be extremely important in early protective responses to mucosal pathogens but, when deregulated, could lead to the development of chronic inflammation, as seen in inflammatory bowel diseases.

Regulation of NF-κB activation is not only dependent on phosphorylation of IκBs but is also dependent on the inducible phosphorylation and transactivation activity of p65 subunit. p65 phosphorylation events occur in the cytoplasm or in the nucleus and are stimuli-specific and, probably, cell-type specific. Atleast three serine residues in p65, namely Ser^{276}, Ser^{529} and Ser^{536} have been shown to undergo phosphorylation by kinases such as protein kinase A (PKA) (Zhong *et al*., 1997), casein kinase II (Kato *et al*., 2003), IKKβ (Ghosh & Karin, 2002) and RSK-1 (Bohuslav *et al*., 2004); these phosphorylations enhance p65's transactivation potential. These findings illustrate a crucial role for p65 phosphorylation in NF-κB activation. However, these p65 phosphorylation data were obtained using different cell lines and it is unclear whether all these p65 phosphorylations occur simultaneously *in vivo* across different cell types. Moreover, it remains to be experimentally demonstrated whether or not p65 phosphorylation on all these sites is required for optimal NF-κB activity.

Utilizing the TMCH model, we demonstrate for the first time that NF-κB activation in hyperproliferating colonic epithelium involves both phosphorylation and degradation of IκBα and phosphorylation of p65 subunit which may facilitate NF-κB's nuclear function. We also demonstrate that p65/RSK-1 and not necessarily p65/IKK interaction may potentially regulate p65 phosphorylation and subsequent NF-κB activation during *C. rodentium* infection.

Methods

Transmissible murine colonic hyperplasia

TMCH was induced in Helicobacter-free Swiss-Webster mice (15–20 g; Harlan) by oral inoculation with a 16-h culture of *C. rodentium*, as previously described (Umar *et al*., 2000a, b, c; 2003). Age- and sex-matched control mice received sterile culture medium only. At appropriate day after exposure to *C. rodentium*, animals were killed, colons were harvested, morphological changes in the colon were determined following staining with hematoxylin and eosin (H&E) as described previously (Umar *et al*., 2000a, b, c; 2003).

Treatment of animals with bortezomib (Velcade®)

Velcade® was purchased from Millennium Pharmaceuticals Inc. (Cambridge, MA, U.S.A.). Both normal and infected mice received Velcade® intraperitoneally (i.p.; at $1\,mg\,Kg^{-1}$ body weight).The treatment groups were: *C. rodentium* infected mice receiving vehicle alone (0.9% sodium chloride); Velcade® injection twice a week for 2 weeks prior to and during *C. rodentium* infection; Normal mice receiving Velcade® injection. Animals in each group tolerated the drug well and weight gain was similar in each group (data not shown). Animals in all the groups were killed 4 h after the last injection, their colons utilized to isolate crypts while a portion of the distal colon from each group was processed for biochemical and immunohistochemical studies as described elsewhere. We have observed significant increases in accumulation of poly-ubiquitinated proteins in response to Velcade® *in vivo* which was due to inhibition of its chymotryptic activity (manuscript under preparation).

Isolation of crypts

Distal colons were attached to a paddle and immersed in Ca^{2+}-free standard Krebs-buffered saline (in $mmol\,l^{-1}$: 107 NaCl, 4.5 KCl, 0.2 NaH_2PO_4, 1.8 Na_2HPO_4, 10 glucose, and 10 EDTA) at 37°C for 10–20 min, gassed with 5% CO_2/95% O_2. Individual crypt units were then separated from the submucosa/musculature by intermittent (30-s) vibration into ice-cold potassium gluconate-HEPES saline (in $mmol\,l^{-1}$: 100 potassium gluconate, 20 NaCl, 1.25 $CaCl_2$, 1 $MgCl_2$, 10 HEPES, 10 glucose, and 5 sodium pyruvate) and 0.1% BSA. Crypts were then concentrated by centrifugation and processed for biochemical analyses.

Subcellular fractionation and protein estimation

Crude cellular homogenates were prepared from crypts isolated from distal colons of normal, *C. rodentium*-infected mice and mice that received Velcade® by homogenization in buffer (50 mM Tris-HCl, 250 mM sucrose, 2 mM EDTA, 1 mM EGTA (pH 7.5), 10 mM 2-mercaptoethanol, 0.5% Triton X-100, plus protease and phosphatase inhibitors). After a

low-speed spin (15 000 × *g* for 15 min), the clear supernatant was saved as total solubilized protein cell extract. Nuclear extracts were prepared from freshly isolated crypts essentially as described by us and elsewhere (Brenner *et al*., 1993; Bohuslav *et al*., 2004). Protein concentrations were determined, and extracts were frozen in liquid nitrogen and stored at −70°C.

Electrophoretic mobility shift assay

Crypt nuclear extracts were prepared from normal or *Citrobacter*-infected mouse distal colon essentially as described (Umar *et al*., 2000a, b, c; Sellin *et al*., 2001). 10 μg of nuclear extract in 10 μl buffer was mixed with 2 μg of poly(dI–dC) and 1 μg BSA to a final volume of 19 μl. After 15- min incubation on ice, 1 μl of [γ-^{32}P] ATP end-labeled double-stranded NF-κB consensus oligonucleotide (TGAGGGGACTTTCCCAGGC) was added to each reaction and incubated at room temperature for an additional 15 min. The reaction products were separated on a 4% native-polyacrylamide-0.5% × Tris-borate-EDTA gel and analyzed by autoradiography. Supershift antibodies (1 μl) were included in the binding reaction as indicated (all supershift antibodies were obtained from Santa Cruz Biotechnology, Santa Cruz, CA, U.S.A.).

Immunoprecipitation and Western blotting

For immunoprecipitation (IP) studies, crypt cytosolic or nuclear extracts were normalized for protein concentration and precleared for 1 h at 4°C with 30 μl of protein A-coated Sepharose beads. IP was carried out at 4°C by incubating the fractions for 2 h with appropriate antibodies and then for 2 h with 50 μl of protein A/G-Sepharose beads. Control experiments were performed by carrying out the IP in the presence of the immunizing peptides, or with control IgG antisera. The immunoprecipitated proteins were recovered by boiling the sepharose beads in 2 × SDS sample buffer.

Total crypt cellular extracts, subcellular fractions (30–100 μg protein/lane) or immunoprecipitated proteins were subjected to SDS–PAGE and electrotransferred to nitrocellulose membrane. The efficiency of electrotransfer was checked by back staining gels with Coomassie blue and/or by reversible staining of the electrotransferred protein directly on the nitrocellulose membrane with Ponceau S solution. No variability in transfer was noted. Destained membranes were blocked with 5% nonfat dried milk in TBS (20 mM Tris-HCl and 137 mM NaCl (pH 7.5)) for 1 h at room temperature (21°C) and then overnight at 4°C. Immunoantigenicity was detected by incubating the membranes for 1–2 h or overnight with the appropriate primary antibodies (0.5–1.0 μg ml^{-1} in Tris-buffered saline (TBS) containing 0.1% Tween 20 (TBS/Tween); Sigma, St Louis, MO, U.S.A.). These antibodies were: polyclonal anti p65, p65-Ser^{536}, IκBα, IκBα-Ser^{32,36}, IKKα/β, IKKα/β-Ser^{176,180}, (Cell Signaling Technology, Beverly, MA, U.S.A.); polyclonal anti p50, laminB (Santa Cruz Biotechnology, Santa Cruz, CA, U.S.A.); mono and polyclonal anti caspase 3 (active), and PCNA (BD Biosciences Pharmingen, San Jose, CA, U.S.A.); monoclonal anti β-actin, RSK-1 (Chemicon International, Temecula, CA, U.S.A.). After washing, membranes were incubated with horseradish peroxidase-conjugated anti-mouse or anti-rabbit secondary antibodies, and developed using the ECL detection system (Amersham Corp., Arlington Heights, IL, U.S.A.) according to the manufacturer's instructions.

Immunohistochemistry

Immunohistochemistry (IHC) for phospho IκBα or p65 was performed on 5-μm-thick frozen sections from distal colons of normal, TMCH and TMCH mice receiving Velcade®, utilizing the HRP labeled polymer conjugated to secondary antibody using Envision + System-HRP (DAB; DakoCytomation, Carpinteria, CA, U.S.A.) with microwave accentuation. Briefly, the sections were heated for 30 min at 65°C, dewaxed in xylene and rehydrated through graded ethanols. Antigen retrieval was performed by heating sections in a microwave in 10 mM sodium citrate buffer (pH 6.0) for 1 min at full power followed by 9 min at medium power. Slides were cooled for 20 min and sections were washed with dH_2O three times for 5 min each. To quench the endogenous peroxidase activity, sections were incubated with peroxidase block for 5 min. After washing, sections were incubated O/N at 4°C with either primary or control antibodies respectively, in a humidified chamber. Incubation with secondary antibody and color development was carried out as per the instructions provided in the kit. Nuclei were stained with hematoxylin. The visualization was carried out using a light microscope.

Results

NF-κB activity increases during TMCH

Infection with *C. rodentium* induced a predictable and reproducible hyperproliferation/hyperplasia in adult Swiss-Webster outbred mouse distal colon at 12 days postinfection with significant increases in crypt length (Figure 1a) with no obvious increase in epithelial or submucosal inflammatory cell numbers as is shown previously (Umar *et al*., 2000a, b, c; 2003). We measured NF-κB activity in the nuclear extracts

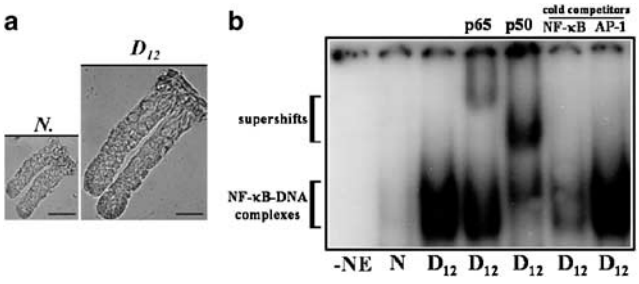

Figure 1 NF-κB activity increases during TMCH: (a) Colonic crypts isolated from normal (N) and day 12 (D_{12}) mucosa exhibited significance increase in crypt length during TMCH (bar = 50 μm; × 400 magnification; $n = 6$). (b) NF-κB activity in nuclear extracts prepared from normal (N) or TMCH crypts (D_{12}) were measured by electrophoretic mobility shift assay (EMSA). NF-κB activity increases dramatically during TMCH (lane 3). Super shift studies were performed by p65 (lane 4) and p50 (lane 5) antibodies, respectively. A DNA competition reaction to show that the NF-κB DNA-binding activity is specific: nuclear extracts prepared from day 12 crypts were incubated with a 50-fold excess of cold competitor DNA containing an NF-κB and AP-1 binding sites (lanes 6 and 7, respectively). Competition for the radioactive NF-κB oligonucleotide binding is observed only with the cold NF-κB oligonucleotide.

prepared from normal or day 12 TMCH crypts by EMSA. NF-κB activity increased dramatically after 12 days of infection (Figure 1b) and exhibited supershifts with antibodies for both p65 and p50 subunits, respectively. Antibodies for p52, c-Rel, and Rel-B, however, failed to shift NF-κB signal (data not shown). Specificity was further established by incubating nuclear extracts with a 50-fold excess of cold competitor DNA containing an NF-κB and AP-1-binding sites. These studies suggest that NF-κB activation during TMCH may be mediated predominantly by p50/p65 heterodimers.

To determine the kinetics of NF-κB activation, we measured (i) NF-κB activity, (ii) p50/p65 and (iii) IκBα protein abundance at different time points during the first 2 weeks after *C. rodentium* infection. NF-κB activity started to increase as early as 3 days after infection and continued to rise over 12-day-period (Figure 2a), paralleling peak hyperplasia. Both p50 and p65 antibodies exhibited corresponding supershifts while cold competition with molar excess of unlabeled probe established the specificity of EMSA studies. When cellular/nuclear levels of p50 and p65 were measured, both p50 and p65 subunits exhibited significant increase in abundance and nuclear translocation during TMCH (Figure 2b), thereby correlating with NF-κB activation kinetics while levels of IκBα decreased significantly during this time (Figure 2c) suggesting existence of a classical pathway of NF-κB activation during TMCH.

In cell lines, stimulation with IL-1 or TNF-α activates a signaling cascade that culminates in the phosphorylation of IκBs. Both IKKα and IKKβ can directly phosphorylate IκBα. However, these kinases themselves undergo phosphorylation in response to the stimulus and are activated in the process. We therefore assessed phosphorylation status of both IKKs during TMCH. As shown in Figure 3, both IKKα and -β exhibited significant increases in phosphorylation while the levels of unphosphorylated IKKs did not change during TMCH. These studies suggest presence of activated IKKs in hyperproliferating crypts which may be involved in regulating IκBα functions *in vivo*.

Phosphorylation of two serine residues at the NH_2-terminus of IκBα ($Ser^{32,36}$) by IKKα/β leads to polyubiquitination and subsequent degradation by the 26S proteasome. While we did not directly measure IKK activity *in vivo*, we set out to determine the phosphorylation status of IκBα during TMCH in order to see whether phosphorylation of IκBα preceded its degradation as reported earlier (see Figure 2c). We chose two time points, day 6 when the hyperplasia first surfaces and day 12, the time of peak hyperplasia, as focal point for initial investigation. Given that IκB phosphorylation particularly that of IκBα, is a transient event and may not be detectable without blocking its proteasomal degradation, the proteasomal activity was inhibited *in vivo* with Velcade®. Frozen tissue sections were then analyzed through IHC to detect presence/absence of phosphorylated IκBα during TMCH. Indeed, proteasomal blockade *in vivo* caused significant accumulation of $Ser^{32,36}$-phosphorylated IκBα on IHC both at day 6 and day 12 TMCH (Figure 4a).

As IκBα is phosphorylated by both IKK catalytic subunits, accumulation of phosphorylated IκBα during proteasomal blockade suggested that Velcade® treatment *in vivo* may not interfere with IKK function during TMCH. Indeed, Velcade® treatment *in vivo* neither affected phosphorylation intensity of either IKKs nor changed the protein levels of unphosphorylated IKKs during TMCH (Figure 4b) paralleling earlier studies (see Figure 3). As blocking degradation of IκBα causes inhibition of NF-κB activation, we next determined the effect of Velcade® on NF-κB activity *in vivo*. Proteasomal blockade *in vivo* led to significant inhibition of NF-κB activity while

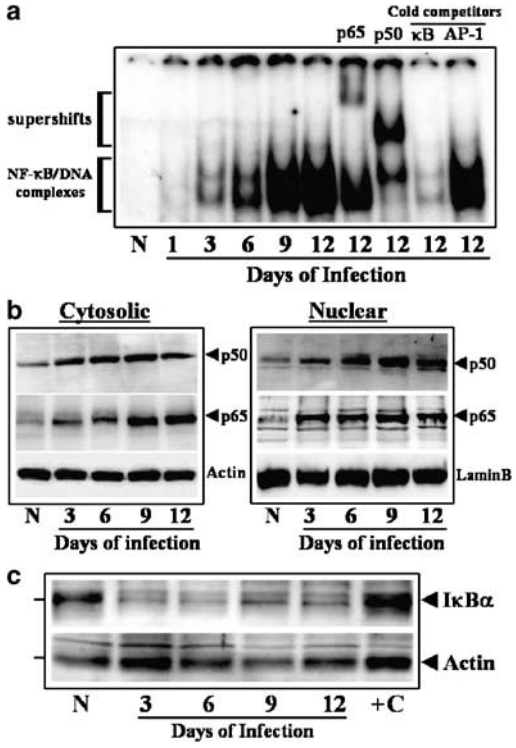

Figure 2 NF-κB/IκBα kinetics. (a) A time course was performed for NF-κB, demonstrating an increased activity as early as day 3 and continued to rise over 12-day-period. Both p65 and p50 antibodies exhibited supershifting of protein–DNA complexes, while cold competition established the specificity of EMSA studies. (b) Cellular and nuclear levels of both p50 and p65 NF-κB subunits increased and paralleled NF-κB activation kinetics. Actin and laminB are loading controls for cytosolic and nuclear extracts, respectively. (c) IκBα degradation preceded NF-κB activation during TMCH. +C is HeLa cell extracts used as positive control.

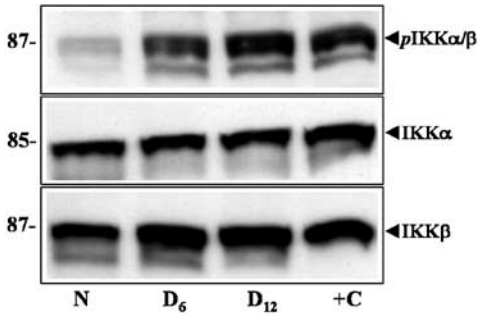

Figure 3 Both IKKα and -β undergo increased phosphorylation *in vivo*. Western blot analysis of total crypt extracts prepared from normal (N), day 6 and day 12 TMCH, revealed significant increases in phosphorylation of both IKKα and -β, compared to control (upper panel) while the levels of unphosphorylated IKKs did not change during TMCH (lower panels). +C is extracts from HeLa cells treated for 5 min with TNF-α and calyculin A and used as positive control.

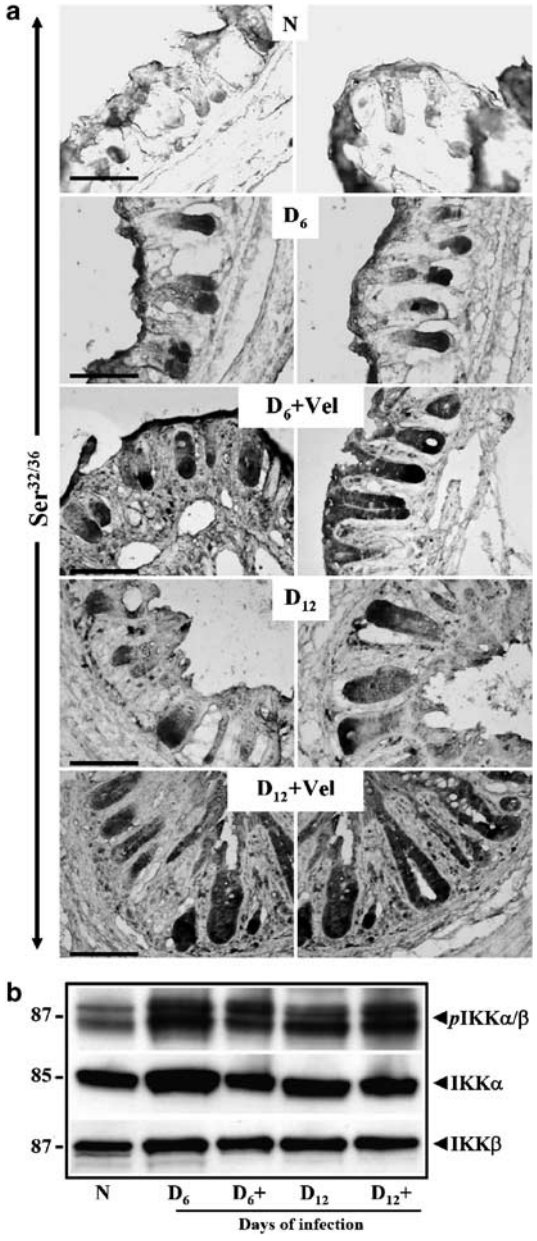

Figure 4 $Ser^{32,36}$-phosphorylated IκBα accumulates after *in vivo* proteasomal blockade. (a) IHC on frozen sections prepared from normal (N), day 6 (D_6), day 6 + Velcade® (D_6 + Vel), day 12 (D_{12}) and day 12 + Velcade® (D_{12} + Vel) TMCH mice Velcade®-treated and untreated distal colons revealed significant accumulation of phosphorylated IκBα both at day 6 and day 12 TMCH, respectively. (bar = 150 μm; $n = 3$). (b) Velcade® neither affected phosphorylation status of IKKs nor changed the protein levels of unphosphorylated IKKs during TMCH. Supplemental material: Concurrently processed crypts in which the primary antibody was replaced with purified mouse IgG, failed to exhibit staining.

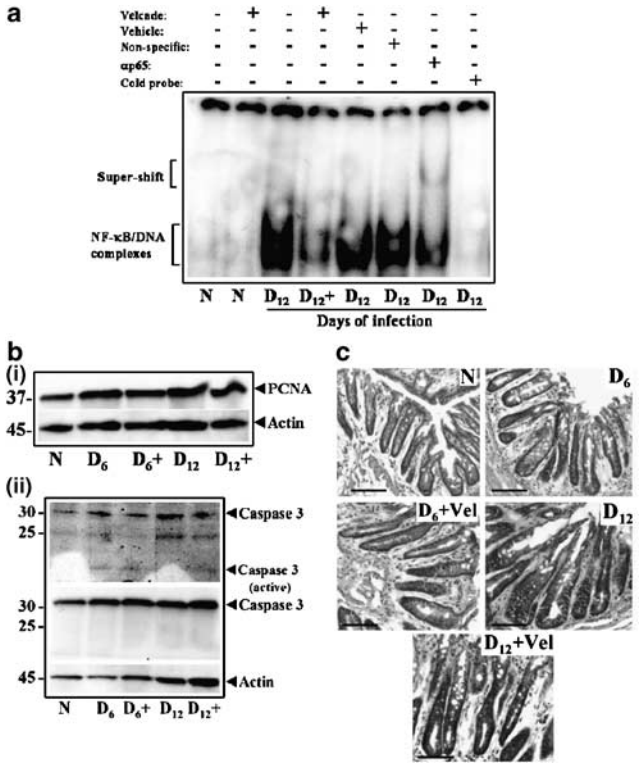

Figure 5 Velcade® blocks NF-κB activity but neither abrogates hyperplasia nor induces apoptosis. (a) EMSA studies were performed in Velcade®-treated normal and day 12 crypt nuclear extracts. Velcade® significantly blocked NF-κB activity at day 12 TMCH while normal animals treated with the same dosage had no effect. Specificity of the gel shift was established both *via* supershift with anti-p65 antibody and by molar excess of cold probe. (bi) Measurement of PCNA abundance in cellular extracts of distal colonic crypts isolated from normal (N) and 6 (D_6), day 6 + Velcade® (D_6 +), day 12 (D_{12}) and day 12 + Velcade® (D_{12} +)-treated distal colons. PCNA abundance was not affected by Velcade®. (bii) Caspase 3 measurement in infected and either treated or untreated samples did not exhibit appearance of activated enzyme even in overexposed gel (upper panel) while total caspase 3, measured with a different antibody, remained unchanged (lower panel). (c) H&E staining of tissue sections prepared from normal (N), day 6 (D_6), day 6 + Velcade® (D_6 +), day 12 (D_{12}) and day 12 + Velcade® (D_{12} +)-treated distal colons. Velcade® did not abolish proliferatory activity of the colonic epithelium as no changes in crypt lengths were noted (bar = 100 μm; $n = 3$).

vehicle alone had no effect (Figure 5a). Intriguingly, NF-κB inhibition *in vivo* neither blocked increases in proliferating cell nuclear antigen (PCNA) abundance (Figure 5bi) nor exhibited increases in appearance of activated caspase 3 even in overexposed gels (Figure 5bii). Total caspase 3 cellular levels therefore did not change in normal, infected or infected + treated samples (Figure 5bii). Inhibition of NF-κB did not abrogate hyperplasia as characteristic findings of TMCH (Umar *et al*., 2000a) were invariably present in the distal colons of treated animals (Figure 5c) indicating that Velcade® does not interfere with *C. rodentium*'s ability to cause hyperplasia. Thus, NF-κB may have additional role(s) besides modulating proliferation *in vivo* during *C. rodentium* infection.

p65 phosphorylation and interaction with CBP/p300: role of ribosomal S6 kinase-1 (RSK-1)

The transcriptional activity of NF-κB can be additionally controlled by various post-translational modifications, including phosphorylation of the p65 subunit at Ser^{536} ($p65^{536}$). Utilizing an antibody specific for $p65^{536}$, we evaluated the phosphorylation status of p65 in both cellular and nuclear extracts during TMCH. A dramatic increase in $p65^{536}$ was observed both at day 6 and day 12 TMCH (Figure 6ai) in crypt

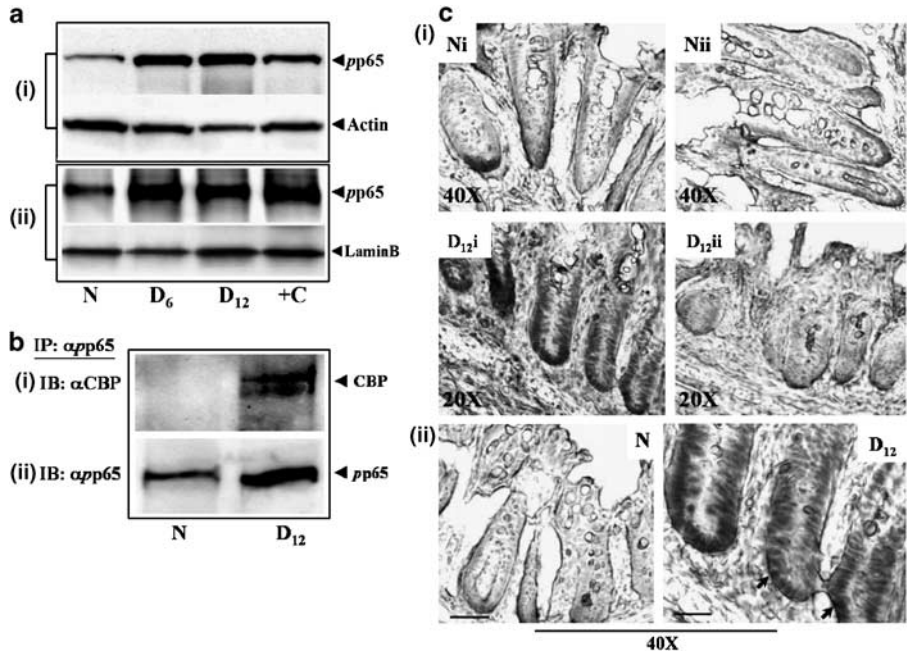

Figure 6 p65 undergoes significant increases in phosphorylation. Total crypt cellular (ai) and nuclear (aii) extracts from normal (N), day 6 (D_6) and day 12 TMCH (D_{12}) distal colon were probed with antibodies for: phospho-Ser^{536} for p65 (p65^{536}), actin and laminB for protein loading. A dramatic increase in cellular p65^{536} both at days 6 and 12, was observed (ai). +C is TNFα-treated HeLa cell extracts used as positive control. p65^{536} also translocated to the nucleus (aii) and interacted with transcriptional coactivator CBP during coIP with αp65^{536} in the nuclear extracts followed by Western blotting with αCBP (b). Lower panel represents blotting with αp65^{536} to confirm presence of p65^{536} in the immunoprecipitates. (c) IHC shows significant nuclear accumulation of p65^{536}during TMCH. Frozen sections prepared from normal (N), day 6 (D_6) and day 12 (D_{12}) mouse distal colon, were stained with anti phospho p65^{536} and analyzed with light microscopy. While normal tissue exhibited barely detectable staining in the crypts, day 12 tissues exhibited dramatic increase in nuclear p65^{536} staining encompassing the entire proliferation zone along the longitudinal crypt axis (ci, bar = 75 μm, N; 100 μm, D_6 and D_{12}, $n = 3$). cii is the 40X version of ci showing detailed nuclear staining at day 12 (arrows).

cellular extracts. p65^{536} also translocated to the nucleus at these time points (Figure 6aii).

We next investigated phosphorylated p65's interaction with transcriptional coactivator CBP. p65^{536} not only translocated to the nucleus but also interacted with nuclear CBP (Figure 6b) suggesting presence of transcriptionally competent NF-κB in the nuclei of hyperproliferating colonic epithelium.

IHC in the frozen sections with p65 antibody specific for Ser^{536} revealed dramatic increases in both cytoplasmic and nuclear staining compared to control. In normally proliferating crypts, cells at the base exhibited weak cytosolic labeling without any nuclear staining (Figure 6ci, Ni). At day 12 TMCH, intense cytoplasmic immunoreactivity extending throughout the longitudinal cellular axis of the crypt alongwith punctate nuclear staining could be seen (Figure 6ci, D_{12}i). Interestingly, the lamina propria was devoid of any immunoreactivity for p65^{536}. Concurrently processed crypts in which the primary antibody was replaced with purified mouse IgG, failed to exhibit staining (Figure 6ci, Nii, D_{12}ii). Figure 6cii is a higher magnification view of 6ci which shows clear nuclear staining in day 12 section (arrows) whereas normal tissue failed to exhibit any nuclear staining.

To delineate a mechanistic basis of NF-κB inhibition following Velcade® treatment, we next looked at presence/absence of activated p65 (p65^{536}) in the nuclei of sections prepared from the distal colons of normal, day 12 and day 12 + Velcade®-treated animals. As shown in Figure 7a, sections from normal distal colon when stained with p65^{536} antibody, exhibited negligible staining. At day 12 TMCH, however, significant p65^{536} nuclear immunoreactivity was recorded (Figure 7) thereby paralleling earlier observation (see Figure 6c). Interestingly, the staining was not limited to

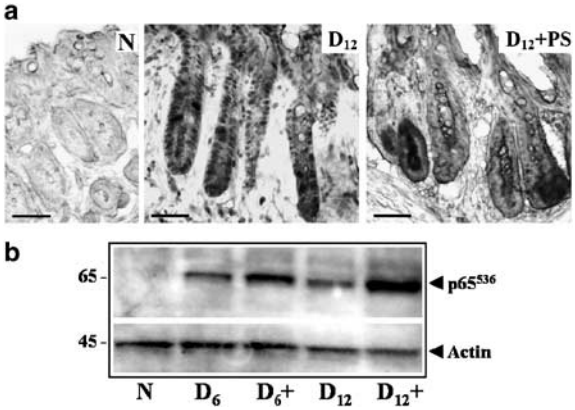

Figure 7 Velcade® mechanistically blocks p65^{536} nuclear translocation. (a). IHC on frozen sections prepared from normal (N), day 12 (D_{12}) and day 12 + Velcade® (D_{12} + PS)-treated distal colons. While significant nuclear staining was observed at day 12, Velcade®-treated tissues exhibited significantly reduced nuclear immunoreactivity at this time point. (b) Phosphorylation status of p65 was not affected by Velcade® (bar = 100 μm; $n = 3$). Supplemental material: Concurrently processed crypts in which the primary antibody was replaced with purified rabbit IgG, failed to exhibit staining.

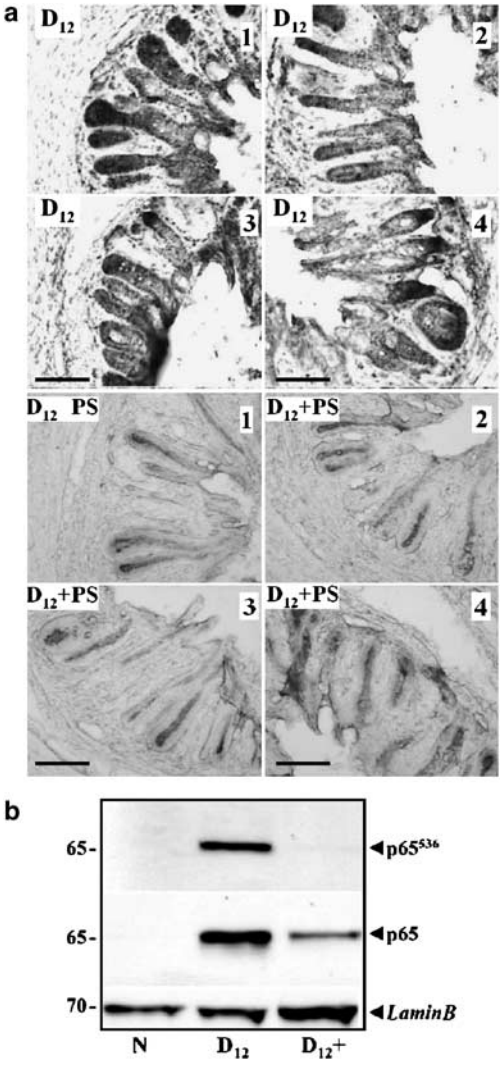

Figure 8 Different regions of the same section exhibit similar staining. (a) IHC on frozen sections prepared from day 12 (D_{12}) and day 12 + Velcade® (D_{12} + PS)-treated distal colons. Positive nuclear staining for $p65^{536}$ was evident in different regions (1–4) of the same sections at day 12 TMCH. Velcade® almost completely blocked $p65^{536}$ nuclear immunoreactivity. [bar = 150 μm; $n = 3$]. (b) Crypt nuclear extracts prepared from normal (N), day 12 (D_{12}) and day12 + Velcade® (D_{12} +)-treated distal colon were probed with antibodies for: $p65^{536}$, p65 and laminB. While day 12 crypt nuclear extracts exhibited significant increases in both $p65^{536}$ and unphosphorylated p65, Velcade® significantly blocked nuclear translocation of both species of p65 paralleling IHC studies.

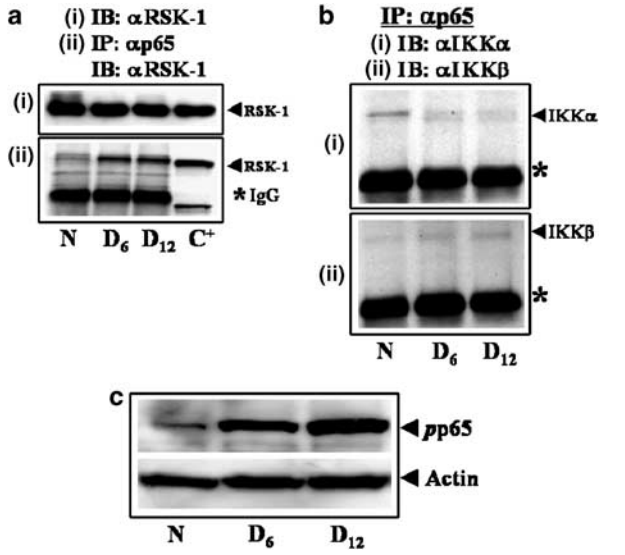

Figure 9 p65 interacts with RSK-1 but not with IKKs. (a) RSK-1 expression analyzed in total crypt extracts prepared from normal (N), day 6 and day 12 TMCH, did not change (i). RSK-1's interaction with p65, however, increased significantly *in vivo* (ii). (b) Co-immunoprecipitation with anti-p65 and blotting with either anti-IKKα (i) or -β (ii) did not reveal any interaction of IKKs with p65. (c) p65/RSK-1 interaction correlated with concomitant increase in cellular $p65^{536}$ during TMCH. *Represents IgG heavy chain while C+ is positive control for RSK-1.

the base of the crypt. Instead, positive nuclear immunoreactivity was observed throughout the longitudinal crypt axis which correlated with expanded proliferative zone in TMCH. Proteasomal blockade *in vivo* led to redistribution of $p65^{536}$ immunoreactivity from the nucleus into the subapical regions of the crypt without significantly reducing its cellular phosphorylation levels (Figure 7b). These results were not only consistent in different regions of the same sections (Figure 8) but also in sections prepared from different animals (data not shown). To determine if Velcade® treatment also affected nuclear translocation of unphosphorylated p65, we performed IHC with antibody recognizing regular p65. Velcade® treatment *in vivo* also reduced movement of unphosphorylated p65 into the nucleus (data not shown).To confirm these findings biochemically, crypt nuclear extracts prepared form normal and day 12 animals either untreated or treated with Velcade® were analyzed for the presence and/or absence of both species of p65. As shown in Figure 8b, Velcade® treatment led to significant block in nuclear translocation of both species of p65 while untreated samples clearly exhibited nuclear translocation of both phosphorylated and unphosphorylated p65, similar to those observed in Figures 2 and 6, respectively. These studies suggest that phosphorylation of p65 may be a cytoplasmic event which may be critical for subsequent nuclear functions of activated NF-κB *in vivo*. This to our knowledge is the first report where effect of an NF-κB inhibitor on nuclear translocation of phosphorylated p65 has been investigated in a native epithelium.

Ser^{536} of p65 can be phosphorylated by the IKKs (Sakurai *et al*., 1999; Jiang *et al*., 2003a, b; O'Mahony *et al*., 2004), but there is also evidence for phosphorylation by serine/threonine kinase ribosomal S6 kinase 1 (RSK-1) (Bohuslav *et al*., 2004). Indeed, alongwith IKKs (see Figure 3), we also detected expression of RSK-1 in cellular extracts of isolated crypts (Figure 9a). Coimmunoprecipitation with anti-p65 and immunoblotting with IKKα/β and RSK-1 revealed significant increases in association of RSK-1 with cytoplasmic p65 both at day 6 and day 12 TMCH, compared to control (Figure 9a) while p65 did not associate with either IKKα or -β at these time points (Figure 9b). The kinetics of RSK-1/p65 interaction correlated with increases in p65 phosphorylation as shown in Figure 9c and elsewhere (see Figure 6). Thus, while it remains to be established whether p65 is a direct target of RSK-1 action *in vivo*, our results suggest that RSK-1 and not necessarily IKKs may be potentially involved in modulating p65 phosphorylation during TMCH.

Discussion

Bacterial attachment enhances the induction of cellular cytokine responses by an unknown mechanism. As many of the genes that are activated in intestinal epithelial cells after bacterial infection are target genes of NF-κB, we investigated the effect of *C. rodentium* infection on NF-κB activation *in vivo*. During *C. rodentium*-induced hyperproliferation/hyperplasia: (a) nuclear translocation of NF-κB in the isolated colonic crypts increased as early as day 3 postinfection and continued to rise for the next nine days paralleling peak hyperplasia, (b) correlating with NF-κB activation, both p65 and p50 subunits exhibited increased abundance in cellular and nuclear extracts while that of IκBα decreased significantly during this time, (c) Phosphorylation of both IKKα (at $Ser^{176/180}$) and -β (at $Ser^{177/181}$) increased significantly during TMCH, (d) Ser^{536} of p65 ($p65^{536}$) underwent increased phosphorylation both at day 6 and 12 TMCH as was revealed by Western blotting and IHC, (e) $p65^{536}$ also translocated to the nucleus and interacted with CBP, (f) proteasomal blockade *in vivo* with Velcade® caused accumulation of $Ser^{32/36}$-phosphorylated IκBα which led to significant inhibition of NF-κB activity *in vivo*, (g) Velcade® also blocked nuclear translocation of activated NF-κB as both immunoblotting and IHC failed to detect any nuclear immunoreactivity for $p65^{536}$, (h) Velcade®, however, did not abrogate hyperplasia, (i) coIP studies revealed significant increases in p65's interaction with ribosomal S6 kinase 1 (RSK-1) but not with IKKα or -β during TMCH.

NF-κB activation during TMCH

NF-κB activation in response to bacterial infection usually involves upstream cellular signals that result in inflammation. Signaling cascades initiated by microbial products culminate in activation of the IκB kinase complex, which phosphorylates inhibitory κB proteins, leading to their degradation (DiDonato *et al*., 1995; Karin & Ben-Neriah, 2000). This enables NF-κB to enter the nucleus, bind to its cognate DNA element and induce target gene transcription. In the present study, we provide a mechanistic basis of NF-κB activation during *C. rodentium* infection *in vivo* that is both (i) dependent on phosphorylation and degradation of IκBα and (ii) relies on post-translational modification of RelA/p65 subunit.

We observed NF-κB activation as early as day 3 postinfection (see Figure 2a) accompanied by concomitant increases in both p65 and p50 protein abundance and nuclear translocation (see Figure 2b). Our supershift studies showed that NF-κB activation during *C. rodentium* infection predominantly involved p50 and p65 heterodimer formation. NF-κB complexes change as colonocytes mature: p65–p50 complexes predominate in proliferating cells while p50–p50 dimer is prevalent in mature epithelial cells (Inan *et al*., 2000). As TMCH is associated with an eight-fold increase in proliferatory index of the colonic epithelium (Umar *et al*., 2000a), our findings correlate with earlier studies and suggest that p65–p50 heterodimerization may be vital in maintaining an activated NF-κB status during TMCH.

Infection of intestinal epithelial cells with microbes or stimulation of cells with proinflammatory cytokines such as IL-1 and TNFα, activates a signaling cascade that leads to phosphorylation of IKK complex at appropriate residues in the activation loop: IKKα at Ser 176 and Ser 180, IKKβ at Ser 177 and Ser 181, respectively. This causes conformational change that leads to their activation. Activated IKKs catalyze phosphorylation of IκBs which earmarks them for degradation (Karin, 1999). We observed significant increases in phosphorylation of both catalytic subunits suggesting presence of activated IKKs in hyperproliferating colonic epithelia. These findings are consistent with studies performed in cell lines where IKKs may play a physiological role in facilitating NF-κB activation in response to bacterial infection (Savkovic *et al*., 1997; Elewaut *et al*., 1999). We also noted IκBα degradation during TMCH and kinetics of degradation correlated with NF-κB activation. Our findings *in vivo* parallel earlier investigations where NF-κB activation follows IκBα degradation during infection with either enteroinvasive or noninvasive bacteria in cell lines (Savkovic *et al*., 1997; Elewaut *et al*., 1999; Haller *et al*., 2002). These studies suggest presence of an activated IKK signaling in hyperproliferating colonic epithelia. While it will be important to determine IKK activity *in vivo* using purified IκBα as a substrate, in the present study, we focused on detecting presence of phosphorylated IκBα as a measure of IKK activation during TMCH.

Phosphorylation of IκBα however, is a transient event and may not be detectable without blocking its proteasomal degradation. Velcade® is a small dipeptidyl boronic acid derivative that binds reversibly to the catalytic threonine and selectively blocks the chymotryptic activity of the 26S proteasome. As 26S proteasome is predominantly involved in the degradation of IκBα, we determined whether blocking proteasomal activity *in vivo* leads to accumulation of phosphorylated IκBα and inhibition of the NF-κB activity. Indeed, proteasomal blockade *in vivo* caused significant accumulation of $Ser^{32,36}$-phosphorylated IκBα as was revealed by IHC (see Figure 4a). This led to significant inhibition of NF-κB activity in Velcade® -treated nuclear extracts (see Figure 5a). These results are consistent with earlier reports in which accumulation of phosphorylated but not nonphosphorylated IκBα was shown to inhibit NF-κB activity *in vivo* (Satou *et al*., 2004).

Phosphorylation of p65 subunit and interaction with CBP/p300: Role of RSK-1

Once activated, inducible post-translational modifications including phosphorylation and acetylation of the p65 subunit allow the regulation of NF-κB transcriptional activity (Zhong *et al*., 1997; Anrather *et al*., 1999; Sizemore *et al*., 1999; Deng *et al*., 2003). Several phosphorylation sites, among them Ser^{536}, are required for p65 activation (Wang & Baldwin, 1998; Madrid *et al*., 2001; Jiang *et al*., 2003a, b). Earlier studies have shown that nonpathogenic Gram-negative *Bacteroides vulgatus* induces transient RelA/p65 phosphorylation, NF-κB activation and proinflammatory gene expression in native and intestinal epithelial cell lines (Haller *et al*., 2002). To test the possibility that the enormous increases in NF-κB activity during TMCH may not be solely dependent on IκBα degradation, we examined the potential role of phosphorylation of Ser^{536} of the p65 transactivating domain 1 (TA1) in modulating NF-κB activity during TMCH.

Phosphorylation of p65 occurs within the cytosolic NF-κB/IκB complex which facilitates phosphorylated p65's nuclear import (Mattioli *et al*., 2004). During TMCH, we observed

significant increases in phosphorylation of cellular p65 at Ser^{536} both at day 6 and day 12, respectively. We also observed nuclear translocation of $p65^{536}$ at both time points suggesting that NF-κB activation during *C. rodentium* infection besides involving IκBα degradation, also requires p65 phosphorylation which may provide additional driving force for nuclear translocation of activated NF-κB. Indeed, in a recent report using mouse epidermal cells, Hu *et al.* (2004) demonstrated that a MEK inhibitor U0126 blocks MEK-1-induced IKK-β activation and p65 phosphorylation at Ser^{536} preventing p65's nuclear import and subsequent interaction with transcriptional coactivator CBP/p300.

For a real-time assessment of this activation therefore, IHC studies were performed in frozen tissue sections prepared from *C. rodentium* infected mice using antibodies specific for Ser^{536}-phosphorylated p65. Our results clearly show significant increases in nuclear immunoreactivity of $p65^{536}$ at peak hyperplasia (see Figures 6c and 8). Thus, phosphorylation of p65 at Ser^{536} may be critical in modulating NF-κB activity during TMCH.

It has been shown previously that phosphorylation of p65 at either Ser^{276} or Ser^{536} following cellular stimulation facilitates NF-κB's nuclear import and recruitment of CBP to the p65 complex for active transcription (Zhong *et al.*, 2002; Hu *et al.*, 2004). This ensures that only stimulus-induced NF-κB activates transcription and NF-κB in the nucleus for any other reason is transcriptionally inactive (Zhong *et al.*, 2002).To determine whether p65/CBP interaction exist *in vivo*, coIP studies were performed in the isolated crypt nuclear extracts of normal and 12 days'-infected animals. Indeed, $p65^{536}$ not only translocated to the nucleus but also interacted with CBP/p300 during TMCH (see Figure 7). Thus, our findings correlate with *in vitro* studies (Zhong *et al.*, 2002; Hu *et al.*, 2004) and suggest presence of a transcriptionally competent protein with ability to recruit coactivator proteins.

We next delineated a mechanistic basis of NF-κB inhibition following Velcade® treatment. Velcade® dramatically reduced nuclear translocation of $p65^{536}$ without significantly altering phosphorylation status of p65 in the cytoplasm (see Figures 7 and 8). These studies suggest that phosphorylation of both p65 and IκBα *in vivo* probably occurs within the cytosolic NF-κB/IκB complex which facilitates degradation of IκBα and subsequent nuclear functions of $p65^{536}$. Phosphorylation of p65 at Ser^{536} has been shown in cell lines to lower its affinity for IκBα leading to $p65^{536}$'s nuclear import (Bohuslav *et al.*, 2004). The fact that $p65^{536}$ nuclear immunoreactivity decreased significantly in Velcade®-treated samples suggests that Velcade®, besides blocking IκBα degradation, may additionally target proteins involved in nuclear import of phosphorylated p65.This is in contrast to *in vitro* studies where proteasome inhibitor MG-132 reduced nuclear translocation of unphosphorylated but not phosphorylated p65 (Sasaki *et al.*, 2005). While to our knowledge, this is the first report of a possible mechanism of NF-κB inhibition after a pharmacological intervention *in vivo*, its important to understand that changes in cellular microenvironment may affect differential responses to a relatively similar approach *in vitro* and *in vivo*.

Blocking NF-κB activity *in vivo*, however, did not abrogate hyperproliferation/hyperplasia suggesting that Velcade® may specifically be blocking NF-κB activation rather than interfering with *C. rodentium's* ability to cause hyperplasia. Moreover, NF-κB's inhibition *in vivo* did not invoke any changes in apoptotic pathway in the colonic mucosa of Velcade® treated animals. These findings suggest that other epigenetic pathways may compensate for the loss of NF-κB in response to Velcade® and may provide survival advantage to hyperproliferating colonic epithelia *in vivo*. We have shown recently that β-catenin is integral to hyperproliferation/hyperplasia observed during TMCH (Sellin *et al.*, 2001; Umar *et al.*, 2003). Although NF-κB and β-catenin signaling pathways are independent, both IκBα and β-catenin are regulated by phosphorylation at similar consensus NH_2-terminal serines leading to targeted ubiquitination and proteasomal degradation. The consequences of this regulation are, however, very different. Indeed, ongoing studies from our lab have shown that proteasomal blockade *in vivo* neither interfered with accumulation of phosphorylated β-catenin nor affected proliferation during TMCH (manuscript in preparation). Given that TMCH is a naturally occurring, self-limiting disease, NF-κB hyperactivity during TMCH, besides exhibiting redundancy with β-catenin, may be additionally required to provide protective immunity to the injured mucosa.

p65 is phosphorylated at Ser^{536} by a variety of kinases *via* various signaling pathways. In most cases, these phosphorylations enhance p65's transactivation potential. Upon stimulation by TNF-α (Sakurai *et al.*, 1999) or the human T-cell lymphotropic virus type 1 Tax protein (O'Mahony *et al.*, 2004), activation of the IKK complex leads to phosphorylation of p65 at Ser^{536}. The IKKβ-mediated phosphorylation of p65 also occurs at Ser^{536} upon T-cell costimulation by the T-cell receptor. Most of these p65 phosphorylations occur upon stimulation by proinflammatory cytokines, but other molecules such as DNA-damaging agents, in addition to their ability to target IκB-α degradation *via* an IKK-independent pathway (Kato *et al.*, 2003), also lead to p65 phosphorylation (Bohuslav *et al.*, 2004). Indeed, drugs such as doxorubicin or etoposide activate NF-κB *via* a p53-dependent pathway that relies on RSK-1-mediated p65 phosphorylation at Ser^{536} (14). We also observed significant increases in p65's interaction with RSK-1 both at day 6 and day 12 TMCH (see Figure 9) with concomitant increase in p65 phosphorylation at Ser^{536}. Thus, p65/RSK-1 interaction and not necessarily p65/IKK interaction may be modulating NF-κB activity during TMCH.

TMCH in context

NF-κB participates in the regulation of cell proliferation and death in many cell types. Its participation in these events has been studied extensively in cell culture, where NF-κB is typically found to promote cell proliferation and suppress apoptosis. However, its role in regulating cell turnover *in vivo* is less well understood.

Our studies have provided novel insights into the mechanistic basis of NF-κB activation in the nonmalignant hyperproliferating crypt. NF-κB activation during TMCH appears to involve both IκBα degradation and p65 subunit phosphorylation which may be critical for NF-κB's nuclear function. Inhibition of the signaling pathways that lead to IκBα degradation prevents NF-κB-dependent gene transcription. Indeed, pharmacological intervention through Velcade® blocked NF-κB activity without significantly altering *C. rodentium*-induced hyperproliferation/hyperplasia. This is in contrast to studies in cell lines where Velcade® blocked cellular growth and promoted apoptosis (Fahy *et al.*, 2003;

Yang *et al*., 2004) while administration of Velcade® into SCID mice bearing tumors suppressed tumor growth (Satou *et al*., 2004). These studies suggest that blocking NF-κB activity alone in situations where redundant epigenetic pathways (e.g., β-catenin; Sellin *et al*., 2001) exist may not be sufficient to block cellular proliferation. Thus, during TMCH, NF-κB may have additional role(s) to perform, for example, in the expression and production of pro-inflammatory cytokines during *C. rodentium* infection and may be even bacterial clearance. Given the potential role of NF-κB in many aspects of tumor development, progression, and therapy, a thorough understanding of the signal transduction pathways that lead to either constitutive (as in cancers), or induced NF-κB activity (e.g., during TMCH), may lead to better prevention strategies.

This work was supported by funds from Crohn's and Colitis Foundation, National Cancer Institute, and the Gastrointestinal Research Interdisciplinary Program (GRIP), UTMB, Galveston, TX.

References

ANRATHER, J., CSIZMADIA, V., SOARES, M.P. & WINKLER, H. (1999). Regulation of NF-kappaB RelA phosphorylation and transcriptional activity by p21(ras) and protein kinase Czeta in primary endothelial cells. *J. Biol. Chem.,* **274,** 13594–13603.

BAEUERLE, P.A. (1991). The inducible transcription activator NF-κB: regulation by distinct protein subunits. *Biochim. Biophys. Acta,* **1072,** 63–80.

BAEUERLE, P.A. & Henkel, T. (1994). Function and activation of NF-κB in the immune system. *Annu. Rev. Immunol.,* **12,** 141–179.

BARTHOLD, S.W., COLEMAN, G.L., BHATT, P.N., OSBALDISTON, G. & JONAS, A.M. (1976). The etiology of transmissible murine colonic hyperplasia. *Lab. Anim. Sci.,* **26,** 889–894.

BARTHOLD, S.W., COLEMAN, G.L., JACOBY, R.O., LIVSTONE, E.M. & JONAS, A.M. (1978). Transmissible murine colonic hyperplasia. *Vet. Pathol.,* **15,** 223–236.

BEG, A.A., FINCO, T.S., NANTERMET, P.V. & BALDWIN JR, A.S. (1993). Tumor necrosis factor and interleukin-1 lead to phosphorylation and loss of IκBα: mechanism for NF-κB activation. *Mol. Cell Biol.,* **13,** 3301–3310.

BOHUSLAV, J., CHEN, L.F., KWON, H., MU, Y. & GREENE, W.C. (2004). p53 induces NF-kappaB activation by an IkappaB kinase-independent mechanism involving phosphorylation of p65 by ribosomal S6 kinase 1. *J. Biol. Chem.,* **279,** 26115–26125.

BRENNER, D.J., GRIMONT, P.A., STEIGERWALT, A.G., FANNING, G.R., AGERON, E. & RIDDLE, C.F. (1993). Classification of Citrobacteria by DNA hybridization: designation of *Citrobacter farmeri* sp. nov., *Citrobacter youngae* sp. nov., *Citrobacter braakii* sp. nov., *Citrobacter werkmanii* sp. nov., *Citrobacter sedlakii* sp. nov., and three unnamed *Citrobacter genomospecies*. *Int. J. Syst. Bacteriol.,* **43,** 645–658.

DENG, W.G., ZHU, Y. & WU, K.K. (2003). Up-regulation of p300 binding and p50 acetylation in tumor necrosis factor-alpha-induced cyclooxygenase-2 promoter activation. *J. Biol. Chem.,* **278,** 4770–4777.

DIDONATO, J.A., HAYAKAWA, M., ROTHWARF, D.M., ZANDI, E. & KARIN, M. (1997). A cytokine-responsive IkappaB kinase that activates the transcription factor NF-kappaB. *Nature,* **388,** 548–554.

DIDONATO, J.A., MERCURIO, F. & KARIN, M. (1995). Phosphorylation of IκBα precedes but is not sufficient for its dissociation from NF-κB. *Mol. Cell Biol.,* **15,** 1302–1311.

DONNENBERG, M.S. & WHITTAM, T.S. (2001). Pathogenesis and evolution of virulence in enteropathogenic and enterohemorrhagic *Escherichia coli*. *J. Clin. Invest.,* **107,** 539–548.

ELEWAUT, D., DIDONATO, J.A., KIM, J.M., TRUONG, F., ECKMANN, L. & KAGNOFF, M.F. (1999). NF-κB is a Central Regulator of the Intestinal Epithelial Cell Innate Immune Response Induced by Infection with Enteroinvasive Bacteria. *J. Immunol.,* **163,** 1457–6614.

FAHY, B.N., SCHLIEMAN, M., VIRUDACHALAM, S. & BOLD, R.J. (2003). AKT inhibition is associated with chemosensitization in the pancreatic cancer cell line MIA-PaCa-2. *Br. J. Cancer,* **89,** 391–397.

GHOSH, S. & KARIN, M. (2002). Missing pieces in the NF-κB puzzle. *Cell,* **109,** S81–S96.

GOOSNEY, D.L., GRUENHEID, S. & FINLAY, B.B. (2000). Gut feelings: enteropathogenic E. coli (EPEC) interactions with the host. *Annu. Rev. Cell Dev. Biol.,* **16,** 173–189.

HALLER, D., RUSSO, M.P., SARTOR, R.B. & JOBIN, C. (2002). IKKβ and phosphatidylinositol 3-kinase/Akt participate in non-pathogenic Gram-negative enteric bacteria-induced RelA phosphorylation and NF-κB activation in both primary and intestinal epithelial cell lines. *J. Biol. Chem.,* **11,** 38168–38178.

HENKEL, T., MACHLEDIDT, T., ALKALAY, I., KRONKE, M., BEN-NERIAH, Y. & BAEUERLE, P.A. (1993). Rapid proteolysis of IκB-α is necessary for activation of transcription factor NF-κB. *Nature,* **365,** 182–185.

HIGGINS, L.M., FRANKEL, G., DOUCE, G., DOUGAN, G. & MACDONALD, T.T. (1999). *Citrobacter rodentium* infection in mice elicits a mucosal Th1 cytokine response and lesions similar to those in murine inflammatory bowel disease. *Infect. Immun.,* **67,** 3031–3039.

HOBBIE, S., CHEN, L.M., DAVIS, R.J. & GALAN, J.E. (1997). Involvement of mitogen-activated protein kinase pathways in the nuclear responses and cytokine production induced by *Salmonella typhimurium* in cultured intestinal epithelial cells. *J. Immunol.,* **159,** 5550–5559.

HU, J., NAKANO, H., SAKURAI, H. & COLBURN, N.H. (2004). Insufficient p65 phosphorylation at S536 specifically contributes to the lack of NF-kappaB activation and transformation in resistant JB6 cells. *Carcinogenesis,* **25,** 1991–2003.

INAN, M.S., TOLMACHEVA, V., WANG, Q.S., ROSENBERG, D.W. & GIARDINA, C. (2000). Transcription factor NF-κB participates in regulation of epithelial cell turnover in the colon. *Am. J. Physiol.,* **279,** G1282–G1291.

JIANG, X., TAKAHASHI, N., ANDO, K., OTSUKA, T. & TETSUKA, T. (2003a). Okamoto T. NF-kappa B p65 transactivation domain is involved in the NF-kappa B-inducing kinase pathway. *Biochem. Biophys. Res. Commun.,* **301,** 583–590.

JIANG, X., TAKAHASHI, N., MATSUI, N., TETSUKA, T. & OKAMOTO, T. (2003b). The NF-kappa B activation in lymphotoxin beta receptor signaling depends on the phosphorylation of p65 at serine 536. *J. Biol. Chem.,* **278,** 919–926.

KARIN, M. (1999). How NF-κB is activated: the role of the IkappaB kinase (IKK) complex. *Oncogene,* **18,** 6867–6874.

KARIN, M. & BEN-NERIAH, Y. (2000). Phosphorylation meets ubiquitination: the control of NF-κB activity. *Annu. Rev. Immunol.,* **18,** 621–663.

KATO JR, T., DELHASE, M., HOFFMANN, A. & KARIN, M. (2003). CK2 Is a C-Terminal IêB Kinase Responsible for NF-êB Activation during the UV Response. *Mol. Cell,* **12,** 829–839.

KENNY, B., LAI, L.C., FINLAY, B.B. & DONNENBERG, M.S. (1996). EspA, a protein secreted by enteropathogenic Escherichia coli, is required to induce signals in epithelial cells. *Mol. Microbiol.,* **20,** 313–323.

LEE, F.S., HAGLER, J., CHEN, Z.J. & MANIATIS, T. (1997). Activation of the IκBα kinase complex by MEKK1, a kinase of the JNK pathway. *Cell,* **88,** 213–222.

LI, Q., VAN ANTWERP, D., MERCURIO, F., LEE, K.F. & VERMA, I.M. (1999a). Severe liver degeneration in mice lacking the IkappaB kinase 2 gene. *Science,* **284,** 321–325.

LI, Z.W., CHU, W., HU, Y., DELHASE, M., DEERINCK, T., ELLISMAN, M., JOHNSON, R. & KARIN, M. (1999b). The IKKbeta subunit of IkappaB kinase (IKK) is essential for nuclear factor kappaB activation and prevention of apoptosis. *J. Exp. Med.,* **189,** 1839b–1845b.

MADRID, L.V., MAYO, M.W., REUTHER, J.Y. & BALDWIN JR, A.S. (2001). Akt stimulates the transactivation potential of the RelA/p65 Subunit of NF-kappa B through utilization of the Ikappa B kinase and activation of the mitogen-activated protein kinase p38. *J. Biol. Chem.,* **276,** 18934–18940.

MATTIOLI, I., SEBALD, A., BUCHER, C., CHARLES, R.P., NAKANO, H., DOI, T., KRACHT, M. & SCHMITZ, M.L. (2004). Transient and selective NF-kappa B p65 serine 536 phosphorylation induced by T cell costimulation is mediated by I kappa B kinase beta and controls the kinetics of p65 nuclear import. *J. Immunol.,* **172,** 6336–6344.

MERCURIO, F., ZHU, H., MURRAY, B.W., SHEVCHENKO, A., BENNETT, B.L., LI, J., YOUNG, D.B., BARBOSA, M., MANN, M., MANNING, A. & RAO, A. (1997). IKK-1 and IKK-2: cytokine-activated IkappaB kinases essential for NF-kappaB activation. *Science,* **278,** 860–866.

O'MAHONY, A.M., MONTANO, M., VAN BENEDEN, K., CHEN, L.F. & GREENE, W.C. (2004). Human T-cell lymphotropic virus type 1 tax induction of biologically Active NF-kappaB requires IkappaB kinase-1-mediated phosphorylation of RelA/p65. *J. Biol. Chem.,* **279,** 18137–18145.

O'NEIL, D.A., PORTER, E.M., ELEWAUT, D., ANDERSON, G.M., ECKMANN, L., GANZ, T. & KAGNOFF, M.F. (1999). Expression and regulation of the human beta-defensins hBD-1 and hBD-2 in intestinal epithelium. *J. Immunol.,* **163,** 6718–6724.

PHILPOTT, D.J., YAMAOKA, S., ISRAEL, A. & SANSONETTI, P.J. (2000). Invasive Shigella flexneri activates NF-kappa B through a lipopolysaccharide-dependent innate intracellular response and leads to IL-8 expression in epithelial cells. *J. Immunol.,* **165,** 903–914.

SAKURAI, H., CHIBA, H., MIYOSHI, H., SUGITA, T. & TORIUMI, W. (1999). IkappaB kinases phosphorylate NF-kappaB p65 subunit on serine 536 in the transactivation domain. *J. Biol. Chem.,* **274,** 30353–30356.

SASAKI, C.Y., BARBERI, T.J., GHOSH, P. & Longo, D.L. (2005). Phosphorylation of RelA/p65 on serine 536 defines an I{kappa}-B{alpha}-independent NF-{kappa}B pathway. *J. Biol. Chem.,* **14,** 34538–34547.

SATOU, Y., NOSAKA, K., KOYA, Y., YASUNAGA, J.-I., TOYOKUNI, S. & MATSUOKA, M. (2004). Proteasome inhibitor, bortezomib, potently inhibits the growth of adult T-cell leukemia cells both in vivo and in vitro. *Leukemia,* **18,** 1357–1363.

SAVKOVIC, S.D., KOUTSOURIS, A. & HECHT, G. (1997). Activation of NF-kappaB in intestinal epithelial cells by enteropathogenic Escherichia coli. *Am. J. Physiol.,* **273,** C1160–C1167.

SCHAUER, D.B., ZABEL, B.A., PEDRAZA, I.F., O'HARA, C.M., STEIGERWALT, A.G. & BRENNER, D.J. (1995). Genetic and biochemical characterization of Citrobacter rodentium sp. *nov. J. Clin. Microbiol.,* **33,** 2064–2068.

SCHERER, D.C., BROCKMAN, J.A., CHEN, Z., MANIATIS, T. & BALLARD, D.W. (1995). Signal-induced degradation of I kappa B alpha requires site-specific ubiquitination. *Proc. Natl. Acad. Sci. USA.,* **92,** 11259–11263.

SELLIN, J.H., UMAR, S., XIAO, J. & MORRIS, A.P. (2001). Increased beta-catenin expression and nuclear translocation accompany cellular hyperproliferation *in vivo*. *Cancer Res.,* **61,** 2899–2906.

SIZEMORE, N., LEUNG, S. & STARK, G. (1999). Activation of phosphatidylinositol 3-kinase in response to interleukin-1 leads to phosphorylation and activation of the NF-kappaB p65/RelA subunit. *Mol. Cell Biol.,* **19,** 4798–4805.

UMAR, S., SCOTT, J., SELLIN, J.H., DUBINSKY, W.P. & MORRIS, A.P. (2000a). Murine colonic mucosa hyperproliferation. I. Elevated CFTR expression and enhanced cAMP-dependent Cl- secretion. *Am. J. Physiol.,* **278,** G753–G764.

UMAR, S., SCOTT, J., SELLIN, J.H. & MORRIS, A.P. (2000b). Murine colonic mucosa hyperproliferation. II. PKC-β activation and cPKC mediated cellular CFTR over-expression. *Am. J. Physiol.,* **278,** G765–G774.

UMAR, S., SELLIN, J.H. & MORRIS, A.P. (2000c). Increased nuclear translocation of catalytically active PKCζ during mouse colonocyte hyperproliferation. *Am. J. Physiol.,* **279,** G223–G237.

UMAR, S., MORRIS, A.P., KOUROUMA, F. & SELLIN, J.H. (2003). Dietary pectin and calcium inhibit colonic proliferation *in vivo* by differing mechanisms. *Cell Prolif.,* **36,** 361–375.

WANG, D. & BALDWIN JR, A.S. (1998). Activation of nuclear factor-kappaB-dependent transcription by tumor necrosis factor-alpha is mediated through phosphorylation of RelA/p65 on serine 529. *J. Biol. Chem.,* **273,** 29411–29416.

YANG, Y., IKEZOE, T., SAITO, T., KOBAYASHI, M., KOEFFLER, H.P. & TAGUCHI, H. (2004). Proteasome inhibitor PS-341 induces growth arrest and apoptosis of non-small cell lung cancer cells via the JNK/c-Jun/AP-1 signaling. *Cancer Sci.,* **95,** 176–180.

ZANDI, E., ROTHWARF, D.M., DELHASE, M., HAYAKAWA, M. & KARIN, M. (1997). The IkappaB kinase complex (IKK) contains two kinase subunits, IKKalpha and IKKbeta, necessary for IkappaB phosphorylation and NF-kappaB activation. *Cell,* **91,** 243–252.

ZHONG, H., MAY, M.J., JIMI, E. & GHOSH, S. (2002). The phosphorylation status of nuclear NF-kappa B determines its association with CBP/p300 or HDAC-1. *Mol. Cell,* **9,** 625–636.

ZHONG, H., SUYANG, H., ERDJUMENT-BROMAGE, H., TEMPST, P. & GHOSH, S. (1997). The transcriptional activity of NF-kappaB is regulated by the IkappaB-associated PKAc subunit through a cyclic AMP-independent mechanism. *Cell,* **89,** 413–424.

(Received February 22, 2006
Accepted April 11, 2006
Published online 5 June 2006)

Supplementary Information accompanies the paper on British Journal of Pharmacology website (http://www.nature.com/bjp)